Development of In-situ Fan Curve Measurement with One Airflow Measurement

Guopeng Liu, Ik-Seong Joo, Li Song, Mingsheng Liu, Ph.D., P.E.
Energy Systems Laboratory
University of Nebraska

ABSTRACT

Fan airflow is the key parameter for air volume tracking control in variable air volume systems. One of the airflow measurement methods is to determine airflow using the fan speed, fan head, and fan curve. Both fan speed and fan head can be measured accurately. Therefore, the accuracy of the fan airflow depends on the accuracy of the fan curve. An experimental method has been developed to determine the in-situ fan curve with only one airflow measurement. This paper presents the theoretical background, experimental procedures, and verification results.

INTRODUCTION

Building pressure control is critical for both occupant comfort and prevention of building structural and systems damage. If the building pressure is improperly controlled or maintained at negative, humid air can leak through the building structure and cause condensation, fungi, and other un-controlled pollution [1]. If the building pressure is too high, it can cause excessive energy cost and unexpected problems. For example, the security door can't be closed due to high building pressure [2]. For a constant air volume system, return air can be properly balanced with supply air properly during the start-up process since the airflows are constant at all times. For a VAV system, supply air flow varies with building load as well as the supply air temperature. To maintain the appropriate positive building pressure, the return air must be properly tracked with the supply air flow. The return airflow should be slightly less than the supply airflow. The difference of the supply and the return airflows depends on the building exhaust airflow and the envelope tightness.

The air volume tracking is often indirectly implemented due to difficulty in obtaining airflow measurements. One of the methods is fan tracking (sometimes referred to as VFD proportional drive-slaving) which resets the return fan speed at or slightingly lagging the supply fan speed. The supply fan is normally controlled by keeping a constant static pressure at some remote point in the ductwork. Both the supply and return fan slow down when less supply air is needed. The problem is that the system flow resistance characteristics change on the supply side (the terminal box dampers) only, but do not change on the return side [1]. This means that the supply fan is running at a different speed and encountering different resistance from the design conditions, hence the airflow is not proportional to speed. However, the return fan *is* operating at a fixed flow resistance. Thus the link between the speeds of the return fan and supply fan cannot maintain correct building pressures except at the point for which the system is balanced [3, 4, 5, and 6].

The second method is the direct building pressure control. The return fan speed is directly controlled to maintain the positive building pressure. If the building is under-pressurized, the return fan slows down so that less return air is drawn back from the space, and less air is sent to the relief air duct. Theoretically this is an excellent solution. But it is very difficult to accurately measure such small static pressure differences as those required for building pressurization (typically 0 Pa (0.00 in. w.g.) to 25 Pa (0.10 in. w.g.) depending on climate [7, 8]). The sensors need to be calibrated, and anecdotal evidence reveals that few facility managers know the location of the pressure sensor. If the pressure sensor is subject to wind, it won't serve its purpose. Also, the pressure may vary throughout the building, particularly in a multi-story building. This method, using existing technology, is extremely difficult to implement [1].

Volumetric tracking [4, 9, 10] measures airflow using flow stations in the main supply duct or the main return duct, or using turbo meters in the fan inlets. The return fan speed is controlled by comparing the flow rates in the supply and return ducts. The fan is modulated to keep this difference at a constant set point, ensuring a constant exfiltration rate (assuming exhaust as a constant). For accuracy within 5 to 10%, a straight, duct for 6-10 duct diameters upstream and 3 duct diameters downstream is required from the airflow measurement station [11].

There are very few systems that have such duct runs in the main supply and return ducts. To increase the accuracy, it is recommended to measure the airflow at the spot with the highest velocity [10]. The fan inlet is such a place. The fan inlet technology measure the airflow at the fan inlet mounted in the intake bell of the fan. However, the airflow profile in the fan inlet varies with the total airflow, which

results in high uncertainties and difficulties of measurement. This method cannot provide the accuracy required for the volumetric tracking, and the cost of the turbo meter is another limitation.

The indirect measurement techniques calculate the airflow from other parameters which are dependent on the flow rate. Most of the indirect measurement techniques use balance equations, such as temperature, concentration, or the enthalpy balance equation. For example, the outside airflow rate can be calculated from the CO_2 concentration levels. The uncertainty of this method is typically high and highly influenced by the concentration difference between the outside and inside air [12]. Moreover, the indirect techniques based on balance equations also require the well-mix of airflow at the measurement locations. Cost is another issue for this method.

Therefore, it is very important to find an effective way to measure the airflow accurately. An airflow control named VSD volumetric tracking (VSDVT) has been developed by Liu [13] recently. This method uses fan airflow station to control the fan airflow. The fan airflow station uses the fan speed and fan head as inputs, with a second-order relationship with fan airflow. The theoretical model has been experimentally tested and excellent agreement between the model and the experimental values was found [1]. The accuracy of the fan airflow station primarily depends on the accuracy of the fan curve since both the fan speed and fan head can be measured accurately.

Typically, the fan curve under full speed can be expressed using second order polynomial equations. The fan curve may be obtained from the manufacturers directly. However, the validity of the manufacture curve may be impacted by the actual fan installation configuration and the actual location of the sensor for the fan head measurement. Therefore, an in-situ measurement may be required. To identify the coefficients of the fan curve, at least three set of data (experiments) should be performed. This traditional method requires extensive modulation of the ductwork resistance to achieve different flow, interrupts the system normal operation, and requires three airflow measurements. The accurate airflow measurement in situ takes significant effort. Therefore, a new method is developed which requires only one air flow measurement and keeps system normal operation. This paper presents the basic theory, experiment procedures, and experiment results.

THEORY AND PROCEDURE

Assuming that the fan curve can be expressed using a second order polynomial equation under full fan speed:

$$H_f = a_0 + a_1 Q_f + a_2 Q_f^2 \quad (1)$$

When the fan is running at another speed, the fan head and the airflow can be correlated using equation (2) according to the fan law.

$$H = a_0 \bar{\omega}^2 + a_1 \bar{\omega} Q + a_2 Q^2 \quad (2)$$

where:

$$\bar{\omega} = \frac{\omega}{\omega_f}$$

To identify the coefficients of the fan curve, at least three experiments should be performed. If the airflow can be maintained at constant during the experiments, the fan curve can be identified by measuring fan head under three different fan speeds.

Assume that the fan has the same airflow Q under three different speeds (ω_0, ω_1, and ω_2). The fan heads are H_0, H_1 and H_2. Introducing these experiments data into Equation 2, a three equation set is generated.

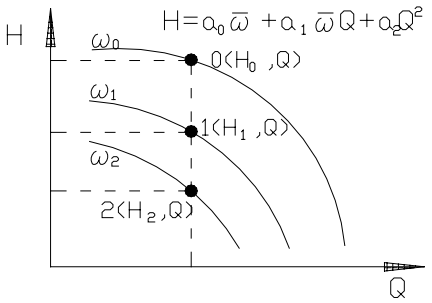

Figure 1. Fan Curve Analysis

$$\begin{cases} H_0 = a_0 \bar{\omega}_0^2 + a_1 \bar{\omega}_0 Q + a_2 Q^2 \\ H_1 = a_0 \bar{\omega}_1^2 + a_1 \bar{\omega}_1 Q + a_2 Q^2 \\ H_2 = a_0 \bar{\omega}_2^2 + a_1 \bar{\omega}_2 Q + a_2 Q^2 \end{cases} \quad (3)$$

From Equation 3, the coefficients of the fan curve can be expressed by:

$$a_0 = \frac{H_0 - H_1}{(\bar{\omega}_0 - \bar{\omega}_1)(\bar{\omega}_1 - \bar{\omega}_2)} - \frac{(H_0 - H_2)}{(\bar{\omega}_0 - \bar{\omega}_2)(\bar{\omega}_1 - \bar{\omega}_2)} \quad (4)$$

$$a_1 = \frac{H_0(\bar{\omega}_2^2 - \bar{\omega}_1^2) + H_1(\bar{\omega}_0^2 - \bar{\omega}_2^2) + H_2(\bar{\omega}_1^2 - \bar{\omega}_0^2)}{Q(\bar{\omega}_0 - \bar{\omega}_1)(\bar{\omega}_0 - \bar{\omega}_2)(\bar{\omega}_1 - \bar{\omega}_2)} \quad (5)$$

$$a_2 = \frac{H_0 \bar{\omega}_1 \bar{\omega}_2 (\bar{\omega}_2 - \bar{\omega}_1) + H_1 \bar{\omega}_0 \bar{\omega}_2 (\bar{\omega}_0 - \bar{\omega}_2) + H_2 \bar{\omega}_0 \bar{\omega}_1 (\bar{\omega}_1 - \bar{\omega}_0)}{Q^2 (\bar{\omega}_0 - \bar{\omega}_1)(\bar{\omega}_0 - \bar{\omega}_2)(\bar{\omega}_1 - \bar{\omega}_2)} \quad (6)$$

As can be seen from Equation (4), the coefficient a_0 is independent of the airflow measurement. When

the coefficients (a_0, a_1, and a_2) and the "design" fan speed (ω_f) are known, the fan airflow can be determined using Equation (7) with measured fan head and fan speed.

$$Q = \frac{-a_1\overline{\omega} - \sqrt{a_1^2\overline{\omega}^2 - 4a_2(a_0\overline{\omega}^2 - H)}}{2a_2} \quad (7)$$

Building heating and cooling loads change smoothly and slowly in large commercial buildings. For a short period, changes in building heating and cooling loads can be neglected. The supply airflow can be approximately considered to be constant during the period when the supply air temperature and main deck static pressure remain unchanged. The return air damper, return fan speed and supply fan discharge flow regulator can be adjusted to achieve different supply fan speeds. Based on this physical process, an innovative fan curve measurement method is developed.

STEP1: Use the maximum return air by closing the relief and outdoor air dampers. During this process, the supply air temperature may change. Wait until the supply air temperature is stabilized before performing the second step.
STEP2: Measure fan airflow, fan head, fan speed, supply air temperature, and static pressure of the AHU. If the fan speed is higher than 70%, go to step 5 directly.
STEP3: Fix return air fan speed and modulate return air damper or an equivalent resistance part gradually to change the supply air fan speed to a preset value, which should be at least 5% higher than the previous value.
STEP 4: Record the fan speed, fan head, static pressure, and supply air temperature. Then repeat steps 3 and 4.
STEP 5: If the fan speed is higher than 70%, decrease the static pressure set point gradually until the fan speed reaches 70%. Go to step 3.
STEP6: Identify the coefficients of the fan curve using Equations 5, 6, and 7.

UNCERTAINTY ANALYSIS

The error propagation was analyzed by using an actual fan curve (see appendix). The measurement uncertainty of sensors in a commercial building was used in the analysis. Assume the relative error of the airflow measurement is 5% in the analysis. The program was developed based on Equation (8) to compute the error propagation. The simulation results show that the interval of the fan speed significantly impacts the accuracy of the fan curve. For example, if the fan speed interval is 20%, the maximum error for the calculated airflow is 5.73%. When the fan speed is adjusted from 75% to 100% (12.5% each time) the maximum airflow error is as high as 10.2%. Therefore, the maximum fan speed interval should be sought during the experiments.

Table 1. the Relative Error Range for the Fan Curve Coefficient and Calculated Airflow

$\overline{\omega}$ (%) fan speed ratio of each points	60%, 80%, 100%	75%, 87.5%, 100%
$\Delta a_0 / a_0$ (%)	0.22%	0.15%
$\Delta a_1 / a_1$ (%)	0.98%	1.7%
$\Delta a_2 / a_2$ (%)	5.88%	2.9%
$\Delta Q'/Q$ (%)	**5.73%**	**10.2%**

EXPERIMENT VERIFICATION

The experiments are carried out at an air-handling unit to test the innovative method and to compare it with the traditional method. The unit serves most of a 247,000 square feet office building in Omaha. The building has two main single duct variable air volume AHUs. Variable frequency drives are installed for each main AHU supply fan (2X125hp) and return air fan (3X40hp). Each AHU serves both interior and exterior zones. A total of 223 terminal boxes supply conditioned air to the space. The supply air fan is controlled to maintain the supply air static pressure. To provide high resistance to increase the supply fan speed, a wood plate was put over the entrance to the supply duct, and the flow resistance was adjusted by moving the plate to regulate the entrance.

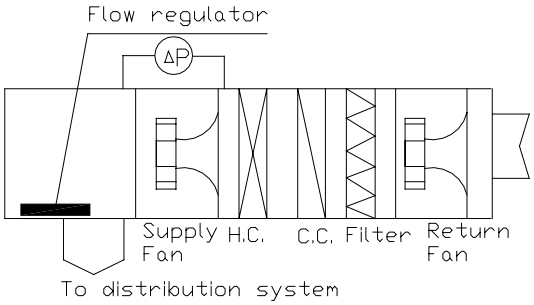

Figure 2. Schematic Diagram of the AHU Used in the Experiment

The supply air fan head is measured using a TSI meter. The differential pressure sensor's range is ±10 inH_2O with an accuracy of ±0.5% reading or ±0.01 inH_2O. Airflows were measured using hot wire flow meters. The measurement range is 30 to 9,999 ft/min with an accuracy 3% reading or 3 ft/min. A five

second interval was set for the average calculation. The fan speed is measured using the variable frequency drive speed.

The fan curve is first measured using the innovative method presented in this paper. Then, the fan curve is measured again using the traditional method, where both air flow and fan head are measured under three different conditions. Finally, six independent measurements were conducted to measure the fan head, fan speed, and fan airflow. Both fan curves obtained from the first and second experiments were used to project the airflow using the measured fan speed and fan head in the independent experiments. The projected airflows are then compared with the measured airflow. The validation of the measured fan curves are then validated using the variance of the projected airflow and the measured airflow in the independent experiments.

Table 2 presents the measured fan head, fan speed, fan airflow, and the supply air temperature for the first experiment, where the fan curve is identified using the innovative method. During the experiment, fan airflow was measured twice in order to confirm that airflow was maintained at the constant level. The variable frequency drive output varied from 58% to 76.2%. The supply air temperature varied from 55.7°F to 56.0°F. The variation is within the error band of the sensor. The airflow varied from 14,637 CFM to 14,786 CFM. The variation is also within the measurement error range. The supply air static pressure was controlled at the constant level. However, the actual values were not recorded during the experiment.

Table 2. Measurement results by one airflow measurement method (method I)

Time	3:25 pm	3:50 pm	4:10 pm
Fan Head (in WG)	2.44	3.13	3.61
Fan Speed (Hz)	34.8 (58%)	39 (65%)	45.7 (76.2%)
Airflow (CFM)	14637	14786	N/A
Supply air temp.(F)	55.7	55.9	56.0

Table3 presents the measured fan speed, fan head, and fan airflow for the second experiment, where the fan curve is identified using the traditional method. The experiments were conducted during a relatively longer period in order to catch the maximum variation of the pressure and airflow that guarantees the three points under different system resistance. The measured fan head varied from 0.55"H_2O to 5.02"H_2O. The fan airflow varied from 5,795 CFM to 32,130 CFM. The fan speed varied from 25% to 94%.

Table 3. Measurement results by typical method (method II)

	Time	Speed ratio [%]	Fan head [in. w.g.]	Air flow rate[CFM]
Point 1	3:25pm 8/29/2003	58	2.44	14637
Point 2	7:55pm 8/29/2003	27	0.55	5795
Point 3	2.55pm 9/03/2003	94	5.02	32130

Table 4 presents the coefficients of the fan curve identified using both experiments 1 and 2. The fan curve coefficients are calculated by Equation (4), (5) and (6) for Method I. The average airflow during the experiment was used to calculate the fan curve coefficients.

Table 4. Fan curve coefficient

	Method I	Method II
a_0	3.238	5.005
a_1	0.0003993	0.0002846
a_2	-9.503E-09	-7.75E-09

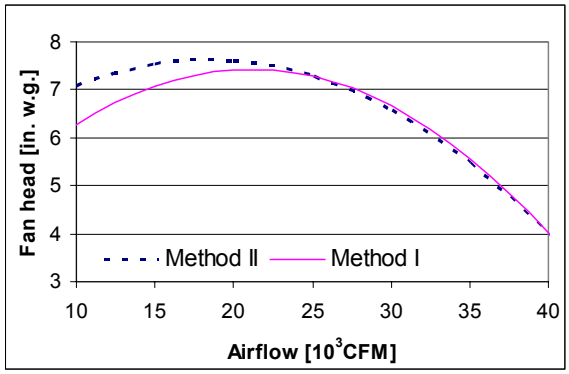

Figure 3. Compares the Fan Curves under the Full Fan Speed

Figure 3 shows the full speed fun curves from two experiments. The two curves agree very well when full speed airflow is higher than 20,000 CFM. Tables 2 and 3 show the experiments were conducted when the corresponding full speed airflow is higher than 19,500 CFM. To ensure accuracy, the regression in-situ fan curve can only apply to the similar working airflow ranges.

Independent airflow measurements were carried out and compared with the airflow calculated by these two groups of fan curves. The calculated airflow can be obtained by the above fan curves, fan heads and fan speeds. The directly measured airflow and calculated airflow values are listed in Table 5. The correlations of directly measured airflow and airflow calculated by in-situ fan curves are shown in Figure 4. Both curves provide satisfactory results. Compared with the directly measured airflow, the mean square root error for method I is 1212 CFM and the mean square root error for method II is 1206 CFM.

Table 5. In-situ Fan Curve Verification

time	3:05 pm 9/2	12:45 pm 8/29	1:28 pm 8/29	1:00 pm 9/3	2:16 pm 9/3
Fan speed ratio %	58.2	36	24.9	60.3	71.3
Fan head In. w.g.	2.49	0.96	1.27	2.68	3.7
Q(M)	14785	9807	10996	13299	16346
Q(I)	14704	8148	11160	14208	17853
Q(II)	14100	8486	11250	14478	17812

Q(M): Directly measured airflow
Q(I): Calculated airflow by fan curve of method I
Q(II): Calculated airflow by fan curve of method II

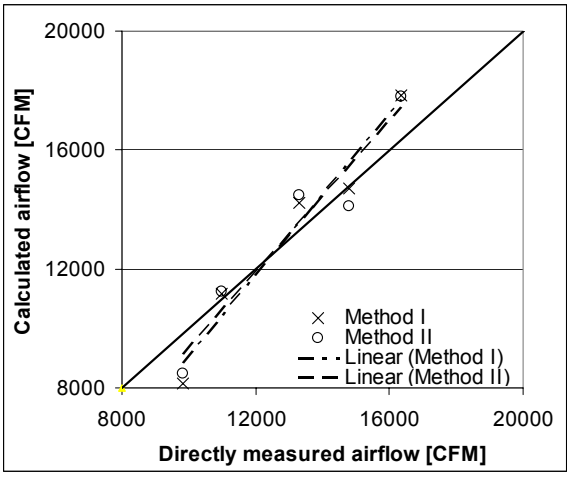

Figure 4. Comparison of Directly Measured and Calculated Airflow

CONCLUSIONS

An experimental method has been proposed and preliminary tested to measure the in-situ fan curve by one airflow measurement. This method takes less time for measurement without influencing the indoor thermal comfort during occupant hours. The preliminary experiment results support the theoretical method, and showed this method provides equivalent accuracy of the traditional measurement method.

The proposed in-situ fan curve measurement method may make the true volume tracking dream come true in the HVAC industry. The experiments method can be further improved to increase the accuracy of the fan curve measurement.

NOMENCLATURE

H Fan head (Pa or inH_2O)
Q Airflow rate (l/s or CFM)
ω Fan speed (RPM)
$\overline{\varpi}$ Speed ratio (%)
Δa_0 Uncertainty of fan curve coefficient a_0
Δa_1 Uncertainty of fan curve coefficient a_1
Δa_2 Uncertainty of fan curve coefficient a_2
$\Delta Q'$ Uncertainty of calculated airflow

Subscripts
f Full speed

REFERENCES:

1. Yuill D. P., Redmann N. K., and Liu M., 2002. "Development of Fan Airflow Station for Airflow Control in VAV Systems"
2. Liu M., Zhu Y., Claridge D.E., and White E., 1997. "Impact of Static Pressure Set Level on HVAC Energy Consumption and Indoor Conditions." ASHARE Transaction 1997, Vol.221, pt. 2.
3. Damiano L. and Dougan D., and Solberg D. W., 1990, " Measurement for the Control of Fresh Air Intake," ASHARE Journal, January 1990, Vol. 32, No. 1, pp.46-51
4. Elovitz D. M., 1995, "Minimum Outside Air Control Methods for VAV systems," ASHARE Transactions, Vol. 101, Pt.2, pp.6133-618
5. Gardner F, T., 1988. "Part load Ventilation deficiencies in VAV systems." Journal of Heating/Piping/Air conditioning, February 1988, pp 89-100
6. Hall J. D., Mudarri D., and Werling E., 1996 "Energy Cost and IAQ Performance of Ventilation Systems and Controls,"

Proceedings of Paths to Better Building Environments, ASHARE, pp. 151-160.
7. Brothers P. W. and Warren M. L., 1986, "Fan Energy Use in Variable Air Volume systems," ASHARE Transactions, Vol. 92, pt. 2B, pp. 19-29
8. Taylor S. T., 2002, "Comparing Economizer Relief Systems," ASHARE Journal, September 2002, Vol. 42, No. 9, pp.32-42.
9. Cohen T., 1994 "Providing Constant Ventilation in Variable Air Volume systems," Proceedings of ASHARE IAQ 93 Conference, Operating and Maintaining Buildings for Health, Comfort, and Productivity, Philadelphia, Pennsylvania.
10. Kettler J. P., 1995, "Minimum Ventilation control for VAV Systems- Fan Tracking vs. Workable solutions," ASHARE transactions, Vol. 101, pt. 2,
11. NEBB, 1986, "Testing Adjusting Balancing manual of Technicians." National Environmental Balancing Bureau.
12. McWilliams J., 2002, "Review of airflow measurement techniques." LBNL-49747, Lawrence Berkeley National Laboratory.
13. Liu M., 2002. "Variable speed drive volumetric tracking (VSDVT) for airflow control in Variable Air Volume (VAV) systems." Journal of Solar Energy Engineering., 2002

APPENDIX:

The most probable error estimate of calculated airflow is generally accepted as the value given by Kline-McClintock's second power relation. The second power relation can be derived from the linearized approximation of the Taylor series expansion of the multivariable function. The propagation of uncertainty in the variables to be result will yield an uncertainty estimate given by

$$\Delta Q' = \pm\sqrt{\left(\left|\frac{\partial Q}{\partial H}\Delta H\right|^2 + \left|\frac{\partial Q}{\partial \bar{\varpi}}\Delta\bar{\varpi}\right|^2\right)} + \left|\frac{\partial Q}{\partial a_0}\Delta a_0\right| + \left|\frac{\partial Q}{\partial a_1}\Delta a_1\right| + \left|\frac{\partial Q}{\partial a_2}\Delta a_2\right| \quad \text{.....(8)}$$

where the sensitive index, results from the Taylor series expansion and is given by

$$\frac{\partial Q}{\partial a_1} = \frac{-\bar{\varpi}Q}{a_1\bar{\varpi} + 2a_2Q} \qquad \frac{\partial Q}{\partial \bar{\varpi}} = \frac{-2\bar{\varpi}a_0 - a_1Q}{a_1\bar{\varpi} + 2a_2Q}$$

$$\frac{\partial Q}{\partial H} = \frac{1}{a_1\bar{\varpi} + 2a_2Q} \qquad \frac{\partial Q}{\partial a_2} = \frac{-Q^2}{a_1\bar{\varpi} + 2a_2Q}$$

$$\frac{\partial Q}{\partial a_0} = -\frac{\bar{\varpi}^2}{a_1\bar{\varpi} + 2a_2Q}$$

a_0, a_1 and a_2 can be calculated by equation (5), (6) and (7), and Q can be calculated by equation (3).The error range Δa_0, Δa_1 and Δa_2 can be calculated by flowing equations

$$\Delta a_0 = \pm\sqrt{\left(\left|\frac{\partial a_0}{\partial H_0}\Delta H_0\right|^2 + \left|\frac{\partial a_0}{\partial H_1}\Delta H_1\right|^2 + \left|\frac{\partial a_0}{\partial H_2}\Delta H_2\right|^2 + \left|\frac{\partial a_0}{\partial \bar{\varpi}_1}\Delta\bar{\varpi}_1\right|^2 + \left|\frac{\partial a_0}{\partial \bar{\varpi}_2}\Delta\bar{\varpi}_2\right|^2 + \left|\frac{\partial a_0}{\partial \bar{\varpi}_0}\Delta\bar{\varpi}_0\right|^2\right)}$$

where the sensitive index, results from the Taylor series expansion and is given by

$$\frac{\partial a_0}{\partial H_0} = \frac{1}{(\bar{\varpi}_0 - \bar{\varpi}_1)(\bar{\varpi}_0 - \bar{\varpi}_2)}$$

$$\frac{\partial a_0}{\partial H_1} = \frac{-1}{(\bar{\varpi}_0 - \bar{\varpi}_1)(\bar{\varpi}_1 - \bar{\varpi}_2)}$$

$$\frac{\partial a_0}{\partial H_2} = \frac{1}{(\bar{\varpi}_0 - \bar{\varpi}_2)(\bar{\varpi}_1 - \bar{\varpi}_2)}$$

$$\frac{\partial a_0}{\partial \bar{\varpi}_1} = \frac{(\bar{\varpi}_0 - 2\bar{\varpi}_1 + \bar{\varpi}_2)(H_1 - H_0)}{(\bar{\varpi}_0 - \bar{\varpi}_1)^2(\bar{\varpi}_1 - \bar{\varpi}_2)^2} + \frac{H_0 - H_2}{(\bar{\varpi}_0 - \bar{\varpi}_2)(\bar{\varpi}_1 - \bar{\varpi}_2)^2}$$

$$\frac{\partial a_0}{\partial \bar{\varpi}_2} = \frac{(\bar{\varpi}_0 - 2\bar{\varpi}_2 + \bar{\varpi}_1)(H_2 - H_0)}{(\bar{\varpi}_0 - \bar{\varpi}_2)^2(\bar{\varpi}_1 - \bar{\varpi}_2)^2} + \frac{H_0 - H_1}{(\bar{\varpi}_0 - \bar{\varpi}_1)(\bar{\varpi}_1 - \bar{\varpi}_2)^2}$$

$$\frac{\partial a_0}{\partial \bar{\varpi}_0} = \frac{1}{(\bar{\varpi}_1 - \bar{\varpi}_2)}\left[\frac{(H_1 - H_0)}{(\bar{\varpi}_0 - \bar{\varpi}_1)^2} + \frac{H_0 - H_2}{(\bar{\varpi}_0 - \bar{\varpi}_2)^2}\right]$$

$$\Delta a_1 = \pm\sqrt{\left(\left|\frac{\partial a_1}{\partial H_0}\Delta H_0\right|^2 + \left|\frac{\partial a_1}{\partial H_1}\Delta H_1\right|^2 + \left|\frac{\partial a_1}{\partial H_2}\Delta H_2\right| + \left|\frac{\partial a_1}{\partial \bar{\varpi}_0}\Delta\bar{\varpi}_0\right|^2 + \left|\frac{\partial a_1}{\partial \bar{\varpi}_1}\Delta\bar{\varpi}_1\right|^2 + \left|\frac{\partial a_1}{\partial \bar{\varpi}_2}\Delta\bar{\varpi}_2\right|^2 + \left|\frac{\partial a_1}{\partial Q}\Delta Q\right|^2\right)}$$

where the sensitive index, results from the Taylor series expansion and is given by

$$\frac{\partial a_1}{\partial H_0} = \frac{(\bar{\varpi}_2 + \bar{\varpi}_1)}{(\bar{\varpi}_0 - \bar{\varpi}_1)(\bar{\varpi}_2 - \bar{\varpi}_0)Q}$$

$$\frac{\partial a_1}{\partial H_1} = \frac{(\bar{\varpi}_2 + \bar{\varpi}_0)}{(\bar{\varpi}_0 - \bar{\varpi}_1)(\bar{\varpi}_1 - \bar{\varpi}_2)Q}$$

$$\frac{\partial a_1}{\partial a_0} = \frac{(\bar{\varpi}_0 + \bar{\varpi}_1)}{(\bar{\varpi}_1 - \bar{\varpi}_2)(\bar{\varpi}_2 - \bar{\varpi}_0)Q}$$

$$\frac{\partial a_1}{\partial Q} = -\frac{H_0(\bar{\varpi}_2^2 - \bar{\varpi}_1^2) + H_1(\bar{\varpi}_0^2 - \bar{\varpi}_2^2) + H_2(\bar{\varpi}_1^2 - \bar{\varpi}_0^2)}{Q^2(\bar{\varpi}_0 - \bar{\varpi}_1)(\bar{\varpi}_0 - \bar{\varpi}_2)(\bar{\varpi}_1 - \bar{\varpi}_2)}$$

$$\frac{\partial a_1}{\partial \bar{\varpi}_0} = \frac{2\bar{\varpi}_0(H_1 - H_2)(\bar{\varpi}_0 - \bar{\varpi}_1)(\bar{\varpi}_0 - \bar{\varpi}_2) - \left[H_0(\bar{\varpi}_2^2 - \bar{\varpi}_1^2) + H_1(\bar{\varpi}_0^2 - \bar{\varpi}_2^2) + H_2(\bar{\varpi}_1^2 - \bar{\varpi}_0^2)\right](2\bar{\varpi}_0 - \bar{\varpi}_1 - \bar{\varpi}_2)}{Q(\bar{\varpi}_0 - \bar{\varpi}_1)^2(\bar{\varpi}_0 - \bar{\varpi}_2)^2(\bar{\varpi}_1 - \bar{\varpi}_2)}$$

$$\frac{\partial a_1}{\partial \bar{\varpi}_1} = \frac{2\bar{\varpi}_1(H_2 - H_0)(\bar{\varpi}_0 - \bar{\varpi}_1)(\bar{\varpi}_1 - \bar{\varpi}_2) + \left[H_0(\bar{\varpi}_2^2 - \bar{\varpi}_1^2) + H_1(\bar{\varpi}_0^2 - \bar{\varpi}_2^2) + H_2(\bar{\varpi}_1^2 - \bar{\varpi}_0^2)\right](2\bar{\varpi}_1 - \bar{\varpi}_0 - \bar{\varpi}_2)}{Q(\bar{\varpi}_0 - \bar{\varpi}_1)^2(\bar{\varpi}_0 - \bar{\varpi}_2)(\bar{\varpi}_1 - \bar{\varpi}_2)^2}$$

$$\frac{\partial a_1}{\partial \bar{\varpi}_2} = \frac{2\bar{\varpi}_2(H_0 - H_1)(\bar{\varpi}_0 - \bar{\varpi}_2)(\bar{\varpi}_1 - \bar{\varpi}_2) + \left[H_0(\bar{\varpi}_2^2 - \bar{\varpi}_1^2) + H_1(\bar{\varpi}_0^2 - \bar{\varpi}_2^2) + H_2(\bar{\varpi}_1^2 - \bar{\varpi}_0^2)\right](2\bar{\varpi}_2 - \bar{\varpi}_0 - \bar{\varpi}_1)}{Q(\bar{\varpi}_0 - \bar{\varpi}_1)(\bar{\varpi}_0 - \bar{\varpi}_2)^2(\bar{\varpi}_1 - \bar{\varpi}_2)^2}$$

$$\Delta a_2 = \pm\sqrt{\left(\left|\frac{\partial a_2}{\partial H_0}\Delta H_0\right|^2 + \left|\frac{\partial a_2}{\partial H_1}\Delta H_1\right|^2 + \left|\frac{\partial a_2}{\partial H_2}\Delta H_2\right| + \left|\frac{\partial a_2}{\partial \bar{\varpi}_0}\Delta\bar{\varpi}_0\right|^2 + \left|\frac{\partial a_2}{\partial \bar{\varpi}_1}\Delta\bar{\varpi}_1\right|^2 + \left|\frac{\partial a_2}{\partial \bar{\varpi}_2}\Delta\bar{\varpi}_2\right|^2 + \left|\frac{\partial a_2}{\partial Q}\Delta Q\right|^2\right)}$$

where the sensitive index, results from the Taylor series expansion and is given by

$$\frac{\partial a_2}{\partial H_0} = \frac{\bar{\varpi}_2 \bar{\varpi}_1}{(\bar{\varpi}_0 - \bar{\varpi}_1)(\bar{\varpi}_2 - \bar{\varpi}_0)Q^2}$$

$$\frac{\partial a_2}{\partial H_1} = \frac{\bar{\varpi}_2 \bar{\varpi}_0}{(\bar{\varpi}_0 - \bar{\varpi}_1)(\bar{\varpi}_1 - \bar{\varpi}_2)Q^2}$$

$$\frac{\partial a_2}{\partial a_0} = \frac{\bar{\varpi}_0 \bar{\varpi}_1}{(\bar{\varpi}_1 - \bar{\varpi}_2)(\bar{\varpi}_2 - \bar{\varpi}_0)Q^2}$$

$$\frac{\partial a_2}{\partial Q} = -\frac{2\left[H_0(\bar{\varpi}_2^2 - \bar{\varpi}_1^2) + H_1(\bar{\varpi}_0^2 - \bar{\varpi}_2^2) + H_2(\bar{\varpi}_1^2 - \bar{\varpi}_0^2)\right]}{Q^3(\bar{\varpi}_0 - \bar{\varpi}_1)(\bar{\varpi}_0 - \bar{\varpi}_2)(\bar{\varpi}_1 - \bar{\varpi}_2)}$$

$$\frac{\partial a_2}{\partial \bar{\varpi}_0} = \frac{\left[(H_1\bar{\varpi}_2(\bar{\varpi}_0 - \bar{\varpi}_2) + H_2\bar{\varpi}_1(\bar{\varpi}_1 - \bar{\varpi}_0)\right](\bar{\varpi}_0 - \bar{\varpi}_1)(\bar{\varpi}_0 - \bar{\varpi}_2) - \left[H_0\bar{\varpi}_1\bar{\varpi}_2(\bar{\varpi}_2 - \bar{\varpi}_1) + H_1\bar{\varpi}_0\bar{\varpi}_2(\bar{\varpi}_0 - \bar{\varpi}_2) + H_2\bar{\varpi}_0\bar{\varpi}_1(\bar{\varpi}_1 - \bar{\varpi}_0)\right](2\bar{\varpi}_0 - \bar{\varpi}_1 - \bar{\varpi}_2)}{Q^2(\bar{\varpi}_0 - \bar{\varpi}_1)^2(\bar{\varpi}_0 - \bar{\varpi}_2)^2(\bar{\varpi}_1 - \bar{\varpi}_2)}$$

$$\frac{\partial a_2}{\partial \bar{\varpi}_1} = \frac{\left[(H_0\bar{\varpi}_2(\bar{\varpi}_2 - \bar{\varpi}_1) + H_2\bar{\varpi}_0(\bar{\varpi}_1 - \bar{\varpi}_0)\right](\bar{\varpi}_0 - \bar{\varpi}_1)(\bar{\varpi}_1 - \bar{\varpi}_2) + \left[H_0\bar{\varpi}_1\bar{\varpi}_2(\bar{\varpi}_2 - \bar{\varpi}_1) + H_1\bar{\varpi}_0\bar{\varpi}_2(\bar{\varpi}_0 - \bar{\varpi}_2) + H_2\bar{\varpi}_0\bar{\varpi}_1(\bar{\varpi}_1 - \bar{\varpi}_0)\right](2\bar{\varpi}_1 - \bar{\varpi}_0 - \bar{\varpi}_2)}{Q^2(\bar{\varpi}_0 - \bar{\varpi}_1)^2(\bar{\varpi}_0 - \bar{\varpi}_2)(\bar{\varpi}_1 - \bar{\varpi}_2)^2}$$

$$\frac{\partial a_2}{\partial \bar{\varpi}_2} = \frac{\left[(H_1\bar{\varpi}_0(\bar{\varpi}_0 - \bar{\varpi}_2) + H_0\bar{\varpi}_1(\bar{\varpi}_2 - \bar{\varpi}_1)\right](\bar{\varpi}_0 - \bar{\varpi}_2)(\bar{\varpi}_1 - \bar{\varpi}_2) + \left[H_0\bar{\varpi}_1\bar{\varpi}_2(\bar{\varpi}_2 - \bar{\varpi}_1) + H_1\bar{\varpi}_0\bar{\varpi}_2(\bar{\varpi}_0 - \bar{\varpi}_2) + H_2\bar{\varpi}_0\bar{\varpi}_1(\bar{\varpi}_1 - \bar{\varpi}_0)\right](2\bar{\varpi}_2 - \bar{\varpi}_0 - \bar{\varpi}_1)}{Q^2(\bar{\varpi}_0 - \bar{\varpi}_1)(\bar{\varpi}_0 - \bar{\varpi}_2)^2(\bar{\varpi}_1 - \bar{\varpi}_2)^2}$$

The accuracy of sensors: The panel mounted digital tachometer with the accuracy ± 0.0015 % of reading. The differential pressure was measured using electromechanical transducer with the accuracy of ± 0.005 in. W.G. and a precision of ± 0.1%. These sensors were used in our measurement. Assume the relative error of the airflow measurement is 3%.

A program was created to compute the relative error range for the airflow calculation. The case is based on a real fan curve of a centrifugal fan

	Point 0	Point 1	Point 2
H(in. W.G.)	0.25	1.25	2.5
ω(RPM)	425	558	701

The airflow was calculated for H= 3 in. WG and ω= 631RPM using equation (7). Then the computed uncertainty was compared with the calculated airflow.

Simulation results:

The relative error for a_0 is 0.22%; the relative error for a_1 is 1.7%, and the relative error for a_2 is 0.98%. The maximum relative error for the calculated airflow is 5.88%.

Assume the relative error of the one airflow measurement is below 1% and the other condition is the same. Therefore, the maximum relative error for the calculated airflow is 2.42%.